The Magnetic Properties of an Electronic Einstein Model Solid

M. F. M. OSBORNE AND M. C. STEELE
Naval Research Laboratory, Washington, D. C.
(Received August 31, 1953)

Following Einstein's proposal for a thermodynamic description of the ions in a solid, we propose a model for the electrons in a solid where the electrons are confined to parabolic wells and, within each well, obey Fermi statistics. The parameters of the model are ω_0, the classical frequency; m, the mass; n_e, the number of particles per well; and n_w, the number of wells per unit volume. In terms of these parameters the magnetic and caloric properties of the model can be unambiguously evaluated. This gives a satisfactory and consistent description of the thermodynamic properties of superconductors and of paramagnetic salts when appropriate values of the above parameters are determined.

I. INTRODUCTION

IT is the purpose of the present paper to devise a model of the electrons in a solid whose magnetic properties give a rough description of real materials, and by rough we mean to the same degree of approximation that an Einstein model of the lattice can be made to describe the lattice specific heat. The Einstein[1] model of the lattice consists of N identical harmonic oscillators and has the property that its specific heat approaches the Dulong-Petit value at high temperatures, whereas below some characteristic temperature it falls rapidly. The parameters of the model are fitted approximately to a real material from physical considerations (elastic constants, atomic masses, volumes, melting point) and represents roughly the behavior of the specific heat in a fairly consistent manner.

The model which we wish to propose for the electrons may therefore be expected, by analogy, to have the following properties. At large fields and high temperatures, we expect the magnetic permeability to approach 1, and the electronic specific heat to be linear, while as field and temperature diminish we would expect the permeability, μ, to approach either 0 (superconducting) or some value greater than 1 (ferromagnetic or paramagnetic). We would expect the electronic specific heat in this region to deviate considerably from a linear law. The parameters of the model would then be adjusted to fit particular real materials as well as possible (just as the Einstein model for the lattice specific heat) so that the transition fields and temperatures from $\mu\sim1$ to $\mu\ll1$, or $\mu>1$, would be approximately as observed.

It should be emphasized that this model as treated in this paper is essentially a thermodynamic one so that such properties as frozen-in moment, remanance, and conductivity cannot be discussed without further assumptions. However, the model itself will suggest how this might be done, just as the Einstein model of a lattice can be used to develop a theory of electrical conductivity[2] and leads to the prediction that the resistivity falls rapidly (but not like T^5 as observed) with decreasing temperature for $T<\Theta$, the Debye temperature.

The model which we propose, therefore, for the "electrons" in a solid is as follows. We imagine that there are n_w parabolic wells of potential $\frac{1}{2}B(x^2+y^2+z^2)$ per unit volume in the solid. In each well we put n_e particles. The particles are of mass m, charge e (taken as the electronic charge), and obey Fermi statistics. Thus, n_w, n_e, B, and m are the parameters of the model which we shall adjust by physical consideration to fit approximately real materials, just as in Einstein's original work. Since n_e determines E_0, the Fermi energy up to which we fill the levels (at $T=0$), we may alternatively use E_0 instead of n_e as a parameter of the model. We will find that for some considerations only the classical frequency in the well $\omega_0=(B/m)^{\frac{1}{2}}$ is the significant parameter so that B and m may not have to be determined separately (a similar situation exists for the Einstein lattice model, of the three parameters N, m, and B only N and ω_0 are needed to determine the specific heat curve). $n_en_w=n$ is the total number of "electrons" per unit volume for the model. We shall see that fitting the model to the physical properties of a real material will either determine the above four parameters or at least give some rather interesting inequalities upon them.

We defer for the moment a justification for this model as well as an estimate on physical grounds of the values of the above parameters. Specifically, the well is not necessarily to be identified with atomic potentials. It will become apparent that the parabolic well has special properties of degeneracy not possessed by an arbitrarily chosen potential, and it is just this degeneracy which is responsible for the properties we derive. The parabolic well has, in addition, the virtue, especially valuable for the problem at hand, that the energy levels can be determined exactly for all values of the magnetic field, so that vexatious perturbation problems in the presence of degeneracy do not have to be considered.

II. SPECIFIC HEAT

A. Case for No Magnetic Field

Let us compute the electronic specific heat of one gram atom (volume A) of material on the basis of this

[1] A. Einstein, Ann. Physik **22**, 180 and 800 (1907).
[2] N. F. Mott and H. Jones, *Theory of the Properties of Metals and Alloys* (Oxford University Press, London, 1936), p. 247.

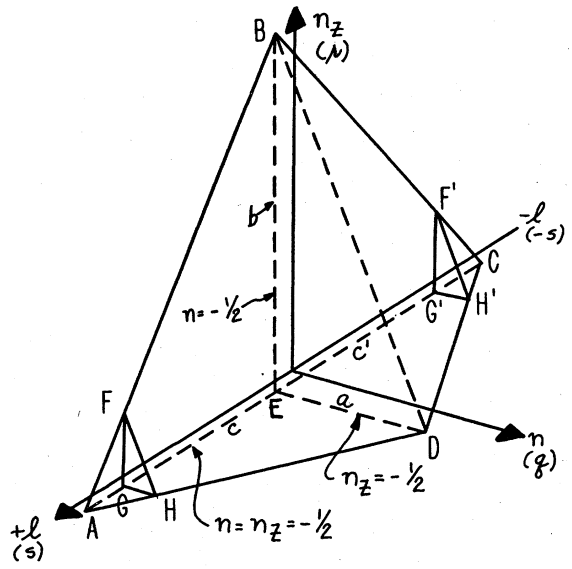

FIG. 1. Constant energy surface in quantum number space for the isotropic oscillator.

model. We shall emphasize certain aspects of this problem and go into considerable detail.

For one well we need, following the development of Seitz,[3] first to compute the number of states less than some arbitrary energy E. This is then combined with the Fermi-Dirac distribution function to compute the relation between E_0, T (temperature), and n_e.

For an isotropic oscillator whose eigenvalues are expressed in the form

$$E=\hbar\omega_0(|l|+2n+n_z+3/2), \tag{1}$$

where $l=0, \pm1, \cdots$; $n=0, 1, 2, \cdots$; $n_z=0, 1, 2, \cdots$, the surface of constant energy in quantum number space is shown in Fig. 1. We wish to compute $N(E)$, the number of points inside or on this surface. For subsequent generality we shall replace the dimensions of Fig. 1 by $ED=a$, $EB=b$, $EA=c$, $EC=c'$. With this notation we have for the isotropic oscillator in the absence of a field [Eq. (1)]

$$b=c=c'=E/\hbar\omega_0, \quad a=E/2\hbar\omega_0. \tag{2}$$

The number of points inside such a pyramid is

$$N(E)=\tfrac{1}{6}ab(c+c')+\sum_{q,r,s\neq0} e^{-\pi i(q+r)}a_{qrs}, \tag{3}$$

where the first term is the volume of Fig. 1 and a_{qrs} are the periodic terms given by

$$a_{qrs}=\int_{\text{Fig. 1}} e^{2\pi i(nq+rn_z+sl)}dndn_zdl. \tag{4}$$

Carrying out the integration gives

$$\begin{aligned}a_{qrs}=\frac{(-1)^{q+r}}{(2\pi i)^3 s}\big[&e^{2\pi irb}\{1/(q-rb/a)(r+sc'/b)\\&-1/(q-rb/a)(r-sc/b)\}\\&+e^{2\pi iaq}\{1/(q+sc'/a)(r-qa/b)\\&-1/(q-sc/a)(r-qa/b)\}\\&+e^{2\pi isc}\{1/(q-sc/a)(r-sc/b)\}\\&-e^{-2\pi isc'}\{1/(q+sc'/a)(r+sc'/b)\}\big].\end{aligned} \tag{5}$$

The origin of energy has been chosen at $n=-1/2$, $n_z=-1/2$.

From geometrical arguments given previously[4] it is evident that for the isotropic oscillator the principal contributions of the periodic part will be from those terms, a_{qrs}, whose indices, q, r, s, are proportional to the direction cosines of the normals to the faces ADB and DCB. This means that the four sets of principal terms will be of the form,

$$a_{2j,j,j}, \quad a_{2j,j,-j}, \quad a_{-2j,-j,-j}, \quad \text{and} \quad a_{-2j,-j,+j},$$

since these directions correspond to catching or missing an entire plane of lattice points on the faces of Fig. 1 as E increases. Substituting the four sets of indices above for q, r, s into Eq. (5) results in an indeterminacy for the isotropic oscillator. This may be resolved by a limiting process or more simply by returning to the defining Eq. (4). The latter procedure gives integrals which are quite straightforward. The resulting expression for $N(E)$ in the case of the isotropic oscillator is

$$\begin{aligned}N(E)=\tfrac{1}{6}(E/\hbar\omega_0)^3+\textstyle\sum_j(-1)^j(E/\hbar\omega_0)^2\\\times\sin[2\pi j(E/\hbar\omega_0)]/2\pi j\\+\text{periodic terms of } O(E/\hbar\omega_0).\end{aligned} \tag{6}$$

This expression is plotted in Fig. 2. The volume term (first term of Eqs. (3) or (6)) is given by the dotted line while the steps represent the contribution of the

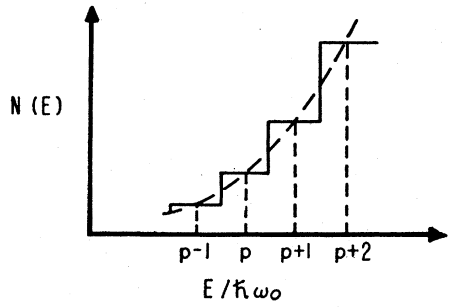

FIG. 2. Number of states within a given energy surface E for the isotropic oscillator in the absence of a field. p is an integer.

[3] F. Seitz, *The Modern Theory of Solids* (McGraw-Hill Book Company, Inc., New York, 1940), p. 150.

[4] M. F. M. Osborne, Phys. Rev. **88**, 438 (1952); M. C. Steele, Phys. Rev. **88**, 451 (1952).

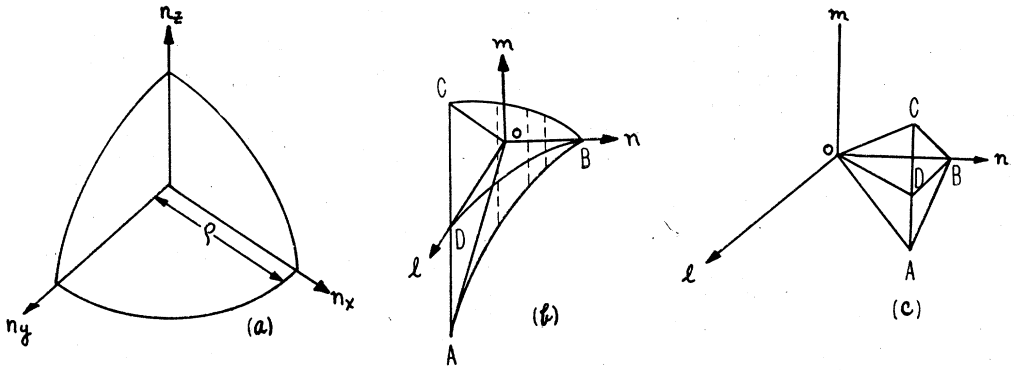

FIG. 3. Constant energy surfaces in quantum-number space for different potentials. (a) Cubical box. (b) Spherical box. ACB is a concave ruled surface and $OD \simeq DC \simeq 2OB$. (c) Coulomb potential $OB \simeq BD \simeq CA/2$.

periodic terms. The height of each riser is the number of points in the two flat faces $ADCB$ of Fig. 1, and the width of the tread is $\hbar\omega_0$.

At this point we wish to comment on the difference between the expression for $N(E)$ for the parabolic well and other types of potential. For the parabolic well the average fluctuation from a smooth curve (the volume term) is of the order of $N(E)^{\frac{1}{3}}$, or the area of a face. For a cubical box of dimension L, the average fluctuation is of order[4]

$$\rho \simeq (2mE)^{\frac{1}{2}}/\hbar L \simeq N(E)^{\frac{1}{3}},$$

where ρ is the radius of curvature in quantum number space (Fig. 3a). For a spherical container, i.e., the potential

$$V=0, \quad r<R, \quad V=\infty, \quad r>R,$$

the constant energy surface is determined by

$$\psi(R)=R^{-\frac{1}{2}}J_{l+\frac{1}{2}}[(2mE/\hbar^2)^{\frac{1}{2}}R]e^{+im\phi}P_l^m(\cos\theta)=0. \quad (7)$$

If n denotes the zeros of the Bessel function, the surface of constant energy[5] in the quantum number space l, m, n is given in Fig. 3b. The average fluctuation of $N(E)$ around a smooth curve is of order $N(E)^{\frac{1}{3}}$. For the Coulomb potential, Fig. 3c, the fluctuation around a smooth curve is of order $N(E)^{\frac{1}{3}}$ just as for the parabolic well. It will be seen that the figures for the highest degeneracy, i.e., the parabolic well and the Coulomb well, correspond to energy surfaces with flat faces whereas the cubical box with a spherical energy surface has the lowest degeneracy. The spherical box has ruled faces instead of flat faces for its constant energy surface and, therefore, falls in an intermediate degeneracy position between these two. The fluctuations for the spherical box are similarly intermediate. Since our previous work has shown that all the magnetic properties must be derivable from these fluctuations, we may expect larger and more interesting magnetic properties to arise from those wells which have the largest degeneracy (flat faces in their surfaces of constant energy in quantum number space), i.e., with the Coulomb or parabolic wells. When kT is less than the spacing of the levels, we may expect departures from the linear specific heat law of a Fermi gas. Furthermore, these departures will be more pronounced as the faces get flatter or the degeneracy increases.

Returning to the computation of the specific heat, we proceed with the condition which determines the Fermi energy, E_0, of one well as a function of T and n_e,

$$n_e=-\int_0^\infty N(E)\frac{df(E)}{dE}dE,$$

where $f(E)$ is the Fermi function. From Eq. (6) this gives

$$n_e=\tfrac{1}{6}(E_0/\hbar\omega_0)^3+\pi^2(kT)^2E_0/6(\hbar\omega_0)^3$$
$$+\mathrm{Im}\sum_{j=1}^{\infty}(-1)^j(E_0/\hbar\omega_0)^2(\exp(2\pi ijE_0/\hbar\omega_0)/2\pi j)$$
$$\times(2\pi^2jkT/\hbar\omega_0)/(\sinh 2\pi^2jkT/\hbar\omega_0)+O(E_0/\hbar\omega_0) \quad (8)$$

in which the first two terms are just those obtained by the conventional method with $N(E)=\frac{1}{6}(E/\hbar\omega_0)^3$ whereas the remaining terms represent the number theory corrections.

Evidently if $kT \gg \hbar\omega_0$, these number theory corrections become negligibly small since they are not only damped exponentially but alternate in sign. In this case the specific heat takes on the conventional expression given by Seitz. For one gram atom of volume A this is

$$C_v=An_w(\pi^2/6)k^2TE_0^2/(\hbar\omega_0)^3. \quad (9)$$

However, with diminishing temperature there must come a point where the effect of the number theory terms can no longer be neglected. In determining the dependence of E_0 on the temperature, however, it has been found impossible, to date, to assess the effect of these corrections [as they appear in Eq. (8)] on E_0 because of the great sensitivity of their contribution to how close $E_0/\hbar\omega_0$ is to an integer. From Fig. 2, which may be considered as the limit of Eq. (8) as $T \to 0$,

[5] E. Jahnke and F. Emde, *Tables of Functions* (Dover Publications, New York, 1945), p. 143.

E_0 is, within the same limits, an indeterminate function of N (or conversely). This is a consequence of degeneracy with the result that fixing E_0 and fixing the number of particles are here (at low temperatures) two different problems (see introduction).

For this reason we have chosen to abandon Eq. (8) at low temperatures ($kT<\hbar\omega_0$) and approach the problem with an approximation which succeeds best at $T=0$ and fails for larger T. This approximation fails at temperatures where the specific heat approximately agrees with the linear law, Eq. (9), so that we can compute the specific heat approximately for all T. Thus, we shall see that except at $T\equiv 0$, this indeterminacy mentioned above can, in fact, be resolved.

We, therefore, first compute by an approximation the specific heat for $kT\ll\hbar\omega_0$, where the number theory correction terms in Eq. (8) obviously dominate. Let us write the expression determining the Fermi energy, E_0, as a function of temperature in its most fundamental form. We denote by Δ_p the number of points in both faces of Fig. 1, and the energy corresponding to any point in either face by $E(p)=\hbar\omega_0(p+3/2)$. Here p is zero or a positive integer. The expression determining E_0 is

$$n_e=\sum_{p\leq p_0}\Delta_p\frac{1}{1+\exp\{[\hbar\omega_0(p+3/2)-E_0]/kT\}}+\sum_{p>p_0}\Delta_p\frac{1}{1+\exp\{[\hbar\omega_0(p+3/2)-E_0]/kT\}},\quad(10)$$

where p_0 is by definition the nearest integer smaller than or equal to $(E_0/\hbar\omega_0)-3/2$. In this form for E_0 we see that n_e is expressed as the sum of terms representing the contribution of states which are full or nearly full ($p\leqq p_0$) plus the contribution of those states which are nearly all empty ($p>p_0$). One or two layers in the immediate neighborhood of the Fermi energy ($p\sim p_0$) have a probability of occupancy near 1/2. We shall need to take explicit account of these.

Now consider in detail the number of particles n_e in one well. This can always be expressed in the form $n_e=N_E(p)+\zeta\Delta_{p+1}$. Here

$$N_E(p)=\sum_{j=0}^{p}\Delta_j$$

is the number of states up to and including the pth layer[5] and ζ is the fraction to which the next face could be filled with particles given the available number n_e. If $\zeta=0$, we speak of a filled face. $\zeta=1/2$ means that 1/2 of the next face could be filled, while $\zeta=1$ would imply that the next face, at $T=0$, would be completely filled. Thus, for the case $\zeta=1$ we could write $n_e=N_E(p+1)$. So we may write

$$n_e=N_E(p_0)+\zeta\Delta_{p_0+1}=\sum_{p\leqq p_0}\Delta_p+\sum_{p\leqq p_0}\Delta_p\times\left[\frac{1}{1+\exp\{[\hbar\omega_0(p+3/2)-E_0]/kT\}}-1\right]+\sum_{p>p_0}\frac{\Delta_p}{1+\exp\{[\hbar\omega_0(p+3/2)-E_0]/kT\}}$$

or, using the definition of $N_E(p)$,

$$\zeta\Delta_{p_0+1}=-\sum_{p\leqq p_0}\frac{\Delta_p}{1+\exp\{[E_0-\hbar\omega_0(p+3/2)]/kT\}}+\sum_{p>p_0}\frac{\Delta_p}{1+\exp\{[\hbar\omega_0(p+3/2)-E_0]/kT\}}.\quad(11)$$

We observe that in this form all of the terms on the right become exponentially small except for perhaps the two or three terms where p is closest to p_0, under the condition that $\hbar\omega_0/kT\gg 1$. Therefore, for sufficiently small temperatures we take into account only the larger terms which are given by those p's closest to p_0. Let us define a function of the temperature $0<\eta(T)<1$ by $(E_0/\hbar\omega_0)-3/2-p_0=\eta(T)$. Then Eq. (11) may be written approximately as

$$\begin{aligned}\zeta\Delta_{p_0+1}\cong&-\Delta_{p_0-1}\frac{1}{\exp[\hbar\omega_0(1+\eta)/kT]+1}&\text{(a)}\\&-\Delta_{p_0}\frac{1}{\exp(\hbar\omega_0\eta/kT)+1}&\text{(b)}\\&+\Delta_{p_0+1}\frac{1}{\exp[\hbar\omega_0(1-\eta)/kT]+1}&\text{(c)}\\&+\Delta_{p_0+2}\frac{1}{\exp[\hbar\omega_0(2-\eta)/kT]+1}.&\text{(d)}\end{aligned}\quad(12)$$

Equation (12) shows that at a sufficiently low temperature, where the Fermi function is sufficiently close to either 0 or 1, only terms (we have taken four) in the immediate neighborhood of the Fermi energy contribute to the temperature dependence of the Fermi energy. Let us now evaluate the specific heat for two limiting assumptions: that the face is either half filled ($\zeta=1/2$) or completely filled ($\zeta=0$).

Evidently for the case $\zeta=0$, if η is near 1/2 (Fermi energy E_0 falling halfway between lattice planes 2, 1, 1), terms (b) and (c) nearly cancel each other whereas (a) and (d) are negligible for kT sufficiently less than $\hbar\omega_0$. For the case $\zeta=0$, therefore, we have approximately, where $\eta(T)=1/2+\epsilon(T)$, $\epsilon(T)\ll 1/2$,

$$0\cong-\Delta_{p_0}/(\exp[(\hbar\omega_0/kT)(\tfrac{1}{2}+\epsilon)]+1)+\Delta_{p_0+1}/(\exp[(\hbar\omega_0/kT)(\tfrac{1}{2}-\epsilon)]+1),\quad(13)$$

[6] It can easily be shown by direct summation that $N(p)=(p^3/6)+p^2+(11p/6)+1$ whence it follows that $\Delta_p=N(p)-N(p-1)=(1/2)p^2+(5/2)p+3$.

from which we find

$$E_0=(p_0+2)\hbar\omega_0-\frac{kT}{\hbar\omega_0}\frac{1}{p_0}[1+\exp(-\hbar\omega_0/2kT)]. \quad (14)$$

The total energy is

$$U=\sum_p(p+3/2)\hbar\omega_0\Delta_p\frac{1}{\exp\{[(p+3/2)\hbar\omega_0-E_0]/kT\}+1}. \quad (15)$$

This can be evaluated in a manner similar to the above derivation for E_0, using only terms corresponding to the layers p_0 and p_0+1 closest to the Fermi energy. Ultimately one obtains for the atomic heat for the case $\zeta=0$ (filled face), using Eqs. (14) and (15),

$$C_{v,\zeta=0}=(\partial U/\partial T)_{\zeta=0}=An_w(k/2)(\hbar\omega_0/kT)^2\Delta_{p0}\exp[-\tfrac{1}{2}(\hbar\omega_0/kT)]\times\{1-2\exp[-\tfrac{1}{2}(\hbar\omega_0/kT)]\}. \quad (16)$$

In a similar fashion it can be shown that for the half filled face, $\zeta=1/2$, the Fermi energy lies almost directly on a lattice plane 2, 1, 1 (probability of occupancy 1/2 at $T=0$). The principal terms in Eq. (12) which have to be taken into account are (b), (c), and (d), and the atomic heat is

$$C_{v,\zeta=\frac{1}{2}}=An_w\frac{\Delta_{p0}170}{81}k(\hbar\omega_0/kT)^2\exp(-\hbar\omega_0/kT). \quad (17)$$

For any other value of ζ (except $\zeta=0$) it can be shown that the Fermi energy for $T\to0$ moves closer and closer to a lattice plane in such a way as to just give a probability of occupancy (the Fermi function) equal to the fraction ζ to which that face is filled, given the available number of particles n_e.

The three expressions for the specific heat, Eqs. (9), (16), and (17), with $p_0=E_0/\hbar\omega_0$, are plotted in dimensionless form against the dimensionless temperature variable $2\pi^2kT/\hbar\omega_0$ in Fig. 4. It will be seen that the two low-temperature approximations agree roughly with the linear law at $2\pi^2kT/\hbar\omega_0\sim3-6$, or roughly at a temperature where one expects them to begin to fail. Thus, together with the linear law they give a description of the specific heat for all temperatures. At very low temperatures the specific heat is vanishingly smaller than the linear law. The filled face case ($\zeta=0$) may rise above the linear law at intermediate temperatures.

B. Case with a Magnetic Field

Now let us consider the effect of a finite magnetic field H on the Fermi surface and its corresponding effect on the specific heat. The energy levels in this case are given[7] by

$$E=\hbar\omega[l+d|l|+d(2n+1)]+\hbar\omega_0(n_z+1/2), \quad \omega=eH/2mc, \quad d=(1+\omega_0^2/\omega^2)^{\frac{1}{2}}, \quad (18)$$

[7] C. G. Darwin, Proc. Cambridge Phil. Soc. **27**, 86 (1931).

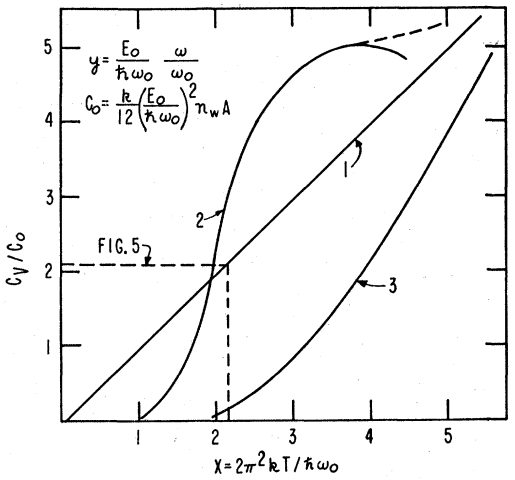

FIG. 4. Specific heat *vs* temperature, both in dimensionless form. (1) Equation (9), linear law, for fields such that $y>1$. (2) Equation (16), no field, filled face ($\zeta=0$, $y=0$). (3) Equation (17), no field, half-filled face ($\zeta=1/2$, $y=0$).

which for small fields, $\omega\ll\omega_0$, takes the form

$$E=\hbar\omega_0[(|l|+2n+1+n_z+1/2)+(\omega/\omega_0)l+\tfrac{1}{2}(\omega/\omega_0)^2|l|+(2n+1)(\omega^2/2\omega_0^2)+O(\omega/\omega_0)^3]. \quad (19)$$

We see that as the magnetic field ($\sim\omega$) increases, the dimensions of Fig. 1 are modified as follows. The l_+ axis decreases linearly with H, the l_- axis increases linearly, and the n axis decreases quadratically (constant to the first order of (ω/ω_0)) in just such a way as to keep the total volume and also the area in the $l-n$ plane a constant. We also note (1) for all fields the Fermi surface is flat, since the energy is linear in the quantum numbers, and (2) that when $(E/\hbar\omega_0)(\omega/\omega_0)<1/2$, the Fermi surface can be placed in such a way as never to cross a lattice plane whereas if $(E/\hbar\omega_0)(\omega/\omega_0)>1/2$, it must do so. That is, if $(E/\hbar\omega_0)(\omega/\omega_0)=1/2$, the Fermi surface has moved by 1/2 unit in quantum number space, inward 1/2 at the end of the l_+ axis, outward 1/2 at the l_- axis (see Fig. 6).

From this we can immediately draw a conclusion about the behavior of the specific heat in a magnetic field large enough that $(E/\hbar\omega_0)(\omega/\omega_0)>1$, in contrast with its behavior in the absence of a magnetic field ($\omega=0$). The departure from the linear law displayed in Fig. 4 is primarily a consequence of the discrete intervals $\hbar\omega_0$ at which the Fermi function is evaluated. Now as soon as $(E/\hbar\omega_0)(\omega/\omega_0)>1$, these intervals are made smaller, being instead $\hbar\omega$ where $\omega\ll\omega_0$. In that case we have a return to the linear law where the specific heat is primarily determined by the volume term in $N(E)$, $\frac{1}{6}(E/\hbar\omega_0)^3$, and only when $\hbar\omega/kT\gg1$ (instead of $\hbar\omega_0/kT\gg1$) can we expect appreciable departures from the linear law, i.e., at much lower temperatures. This is indicated by the straight line (1) of Fig. 4. Thus, the effect of a magnetic field appreciably greater than a certain critical value [i.e., when $(E/\hbar\omega_0)(\omega/\omega_0)=1$] is

to make the specific heat linear to much lower temperatures.

The way in which curves (2) and (3) of Fig. 4 distort into (1) as the field increases, up to $(E/\hbar\omega_0)(\omega/\omega_0)=1$, can be evaluated approximately as follows. From Eq. (19) the energy levels within the pth layer may be written [neglecting $(\omega/\omega_0)^2$] as

$$E(p)=(p+3/2)\hbar\omega_0+l\hbar\omega. \tag{20}$$

One then evaluates the specific heat by using only the contribution of the layers nearest to the Fermi energy, exactly as in the development which led to Eq. (12), where instead of Δ_p, Δ_{p+1}, etc., we now have a summation (which can be replaced by an integral if $kT/\hbar\omega>1$), over each layer. Since the correction $l\hbar\omega$ [Eq. (20)] to the energy of a state within a given layer does not depend on n or n_z, this means that we can replace the integration over a layer by its projection on the l, n, plane. This gives for the case of a half-filled face

$$C_{v,\zeta=\frac{1}{2}}=(2\pi^2kT/\hbar\omega_0)n_wA\,(k/6)\,(E_0/\hbar\omega_0)^2\times(1/2)\,(\omega_0/\omega)\,(\hbar\omega_0/E_0),$$
$$\text{valid if } kT/\hbar\omega_0\ll(E_0/\hbar\omega_0)(\omega/\omega_0),\quad \hbar\omega\ll kT\ll\hbar\omega_0,\quad (E_0/\hbar\omega_0)(\omega/\omega_0)<1. \tag{21}$$

For the filled face case we find

$$C_{v,\zeta=0}=\pi^2(k^2T/3)n_wA\,(1/\hbar\omega)\times\left[\left(\frac{E_0}{\hbar\omega_0}\right)\left(\frac{\omega}{\omega_0}\right)-\frac{1}{2}\right](E_0/\hbar\omega_0),$$
$$\text{valid if } 1>(E_0/\hbar\omega_0)(\omega/\omega_0)>1/2 \tag{22}$$

and

$$kT\ll\left[(E_0/\hbar\omega_0)(\omega/\omega_0)-\tfrac{1}{2}\right](E_0/\hbar\omega_0)\hbar\omega.$$

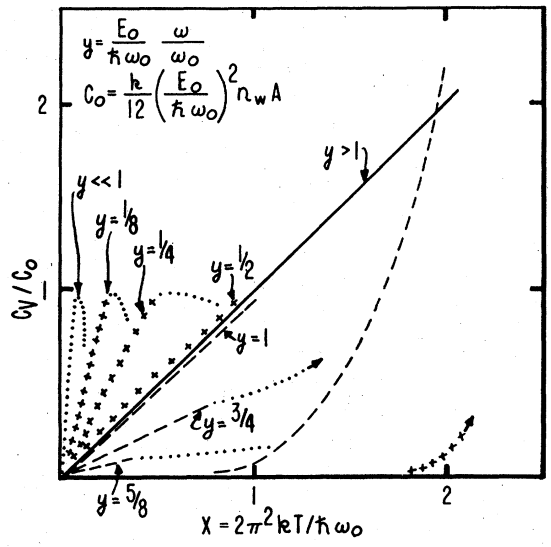

FIG. 5. Specific heat *vs* temperature, in dimensionless form, for different values of the dimensionless magnetic-field variable y. Full curve, linear law for high temperatures and $y>1$. Dashed line, filled face ($\zeta=0$). Crosses, half-filled face ($\zeta=1/2$). Dotted lines indicate estimated behavior beyond the validity range of the formulas.

These formulas essentially use the conventional expression for the specific heat, $(\pi^2/3)[k^2Tg(E_0)]$, where the density of states $g(E)$ is that "seen" by the Fermi energy (E_0) as it crosses a lattice plane, and T is so small that neither the extreme values of energy at the ends A, C of the lattice planes of Fig. 1 nor adjacent lattice planes have any contribution.

For higher temperatures both of these specific heats must approach the high-temperature linear law. However, for very weak fields there is a limited range in T over which $C_{v,\zeta=\frac{1}{2}}$ falls like $1/T^2$, corresponding to the narrow-band approximation of Mott and Jones.[2] This condition is realized when kT is much greater than $(2E_0/\hbar\omega_0)\hbar\omega$, the energy width of a single face of Fig. 1, but much less than $\hbar\omega_0$, the spacing of lattice planes. Thus, the specific heat for the case of a half-filled face develops a thin spine near $T=0$ which for increasing H broadens and flattens into the high-temperature linear law. The entropy given by the integral of $dS=C_vdT/T$ over this spine (see Sec. VI, B) is essentially constant and represents the zero-point entropy of the half-filled face case since at the absolute zero the well, considered as a single system, has a degeneracy given by the number of ways the face may be half filled.

For the filled-face case the specific heat near $T=0$ rises steadily to the linear law as the field is increased. The bump on curve (2) of Fig. 4 probably moves to lower temperatures with increasing field, although we have not been able to verify this. Figure 5 shows a dimensionless plot of Eqs. (21) and (22).

III. EVALUATION OF THE MOMENT AT $T=0$°K

Let us first consider the behavior of the Fermi energy at temperatures so small that the criterion $\hbar\omega/kT\gg1$ is observed. This is the condition for the Fermi function to drop from one to zero in the interval between adjacent energy levels [see Eq. (20)]. This will not be essentially different from the behavior as $T\to0$. For the case of a filled face we saw that for $H=0$ the Fermi energy huddled up to the plane bisecting the space between two lattice planes whereas for a partly filled face, in particular for $\zeta=1/2$, it has to huddle up to a lattice plane in just such a way as to preserve (give a probability of occupancy of) the appropriate fraction of that face.

So we can see that for $(E/\hbar\omega_0)(\omega/\omega_0)<1/2$, if we order the states in terms of increasing energy, they fall in the order indicated in Fig. 6. Each layer starts at $-l$ and increases in energy to $+l$. After a layer is filled, one starts to fill the next layer at $-l$. We now ask how the Fermi energy behaves as H increases. Evidently if at some field H the Fermi surface passes between say the points 8, 9 of Fig. 6 (face more than half full), as H increases further, E_0 must increase just enough to make the Fermi surface always pass between these same two points so that in summing the Fermi function in $n_e=\sum_i f(E_i,E_0)$, one counts essentially all the points inside and none outside in order to preserve n_e.

For a face less than half full (if E_0 passes between 5 and 6 of Fig. 6), E_0 must decrease with increasing H. Ultimately, (for $(E/\hbar\omega_0)(\omega/\omega_0)>1$) since the Fermi *volume* does not change with H, E_0 must oscillate ($\sim\hbar\omega$) with H just enough to enclose always exactly the same number of points (having the lowest energy). Precisely and only for the cases $\zeta=0$ and $\zeta=1/2$, E_0 need not change [neglecting $(\omega/\omega_0)^2$] with H at all even in the range $(E/\hbar\omega_0)(\omega/\omega_0)<1/2$, since for these two values of the face filling the Fermi surface, for fixed E_0 and changing H, either does not cut lattice planes at all ($\zeta=0$), cuts them always at the same point ($l=0$ if $\zeta=1/2$), or loses and gains lattice points in equal amounts (starting at the ends of the 1 axis) as the field varies.

With this understanding, and at extremely low temperatures ($kT\ll\hbar\omega$), we can, therefore, evaluate the magnetic moment from

$$\begin{aligned}M&=-(\partial F/\partial H)_{E_0}\\&=(\partial/\partial H)_{E_0}\textstyle\sum_i kT\ln\{1+\exp[(E_0-E_i)/kT]\}\\&=-\sum_{E_i\leq E_0}(\partial E_i/\partial H)+kT(\partial/\partial H)\\&\quad\times\sum_{E_i\leq E_0}\exp[-(E_0-E_i)/kT]\\&\quad+kT(\partial/\partial H)\sum_{E_i>E_0}\exp[(E_0-E_i)/kT]\\&\quad+\sum_{E_0\lesssim E_i}O\exp[\pm 2(E_0-E_i)/kT],\end{aligned}\tag{23}$$

where we understand that E_0 is so adjusted with H that the Fermi surface always encompasses exactly the same number and set of points so long as $(E_0/\hbar\omega_0)(\omega/\omega_0)<1/2$. For still larger fields E_0 can be considered as approximately constant (independent of H) since for every point lost on the $+1$ face, another will be gained on the -1 face.

If the temperature is sufficiently low ($kT\ll\hbar\omega$), we can drop all but the first term of Eq. (23) and then evaluate the summation of the first term (for some purposes an integral will here suffice). For a half-filled face we sum for finite H over the interior volume and the $-l$ face, DCB, Fig. 1, whereas for the filled face we sum over the interior volume and both faces. This procedure is valid provided we satisfy the inequality $(E/\hbar\omega_0)(\omega/\omega_0)<1/2$ if $\zeta=0$, or $(E/\hbar\omega_0)(\omega/\omega_0)<1$ for $\zeta=1/2$. This results in the following expressions for the moment per unit volume (n_w wells per cc). It should be noted that for the filled face ($\zeta=0$) summing (but not integrating) cancels exactly the $l\hbar\omega$ terms in Eq. (19) so that we must carry terms in ω^2/ω_0^2. These may be integrated. Also, for $\zeta=1/2$, we must sum the $-l$ face (or integrate it as a projected area DEC) and *not* integrate it as a thin three-dimensional wedge since a point in this face, when counted, is counted at full weight.

$$M(T=0,\zeta=0)=-n_w(1/12)(e\hbar/2mc)(\omega/\omega_0)(E_0/\hbar\omega_0)^4,\quad\text{valid if }(E_0/\hbar\omega_0)(\omega/\omega_0)<1/2;\tag{24}$$

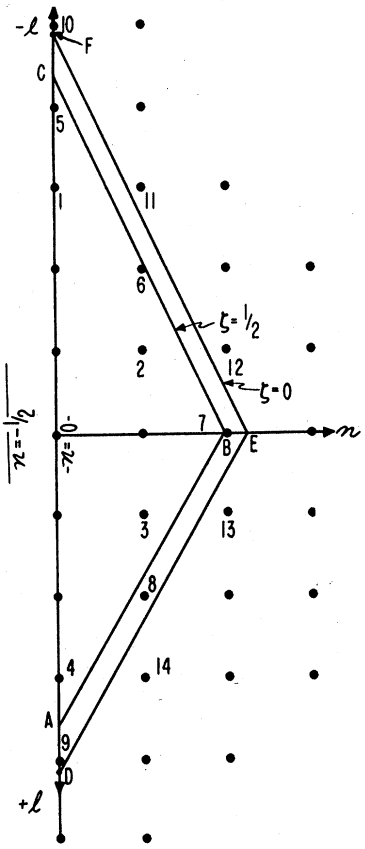

FIG. 6. Constant energy contour in n, l plane for small, finite field H. ABC corresponds to case of half-filled face, which neither loses nor gains points as long as $y=(E/\hbar\omega_0)(\omega/\omega_0)<1$. DEF corresponds to filled-face case which neither loses nor gains points for $y<1/2$.

$$M(T=0,\zeta=1/2)=+(n_w/12)(E_0/\hbar\omega_0)^3(e\hbar/2mc)-(n_w/12)(e\hbar/2mc)(\omega/\omega_0)(E_0/\hbar\omega_0)^4,\quad\text{valid if }(E_0/\hbar\omega_0)(\omega/\omega_0)<1.\tag{25}$$

These are plotted in Fig. 7.

We may carry the analysis for the case of a filled face outside the range $(E_0/\hbar\omega_0)(\omega/\omega_0)<1/2$, still taking into account that the temperature is so small that the Fermi function drops from one to zero in the range ($\hbar\omega$) between points in a face and just include the contributions of the first term in Eq. (23) appropriately. We thus obtain the segment AB of Fig. 7, where the change in slope at A indicates that the Fermi surface is just catching or missing one of the lattice planes $2j$, j, $\pm j$. The range over which $\partial E_i/\partial H$ is summed is the interior and surface of Fig. 1, minus a triangular patch (points lost) AFH (projected to AGH), plus a patch $F'H'C$ (projected to $H'G'C$) of points gained in the next outer lattice plane. The dimension $AG=G'C$ is $(E/\hbar\omega_0)-(\omega_0/2\omega)$. This gives for the moment per unit volume for the case of a filled face in the range

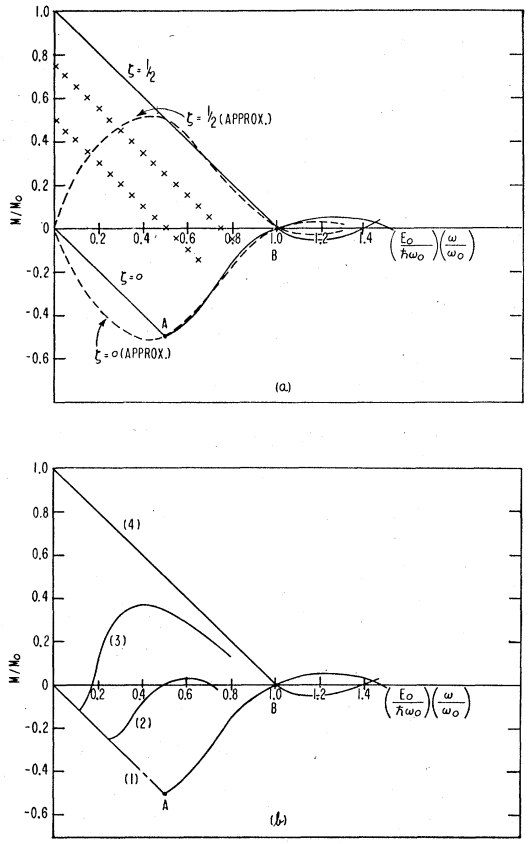

FIG. 7. Dimensionless magnetization as a function of dimensionless field at $T=0$. $M_0=n_w\beta(E_0/\hbar\omega_0)^3/12$. (a) Number of particles, n_e, fixed. Full curves, exact [Eqs. (24), (25) (26)]; ---- one term approximation [Eq. (31)]; xxxx, moment for fillings intermediate between filled and half filled. (b) Fermi energy fixed. (1) and (4) are identical with the filled and half-filled full curves of (a) and correspond to $E_0/\hbar\omega_0=p$ and $E_0/\hbar\omega_0=p+(1/2)$ (where p is an integer), respectively; (2) $E_0/\hbar\omega_0=p+(1/4)$; (3) $E_0/\hbar\omega_0=p+(3/8)$.

$$1/2<(E_0/\hbar\omega_0)(\omega/\omega_0)<1$$

$$M(T=0,\zeta=0)=-n_w[(1/12)(e\hbar/2mc)(\omega/\omega_0)(E_0/\hbar\omega_0)^4+(1/8)(e\hbar/2mc)(E_0/\hbar\omega_0)(\omega_0/\omega)^2-(1/6)(E_0/\hbar\omega_0)^3(e\hbar/2mc)-(1/24)(e\hbar/2mc)(\omega_0/\omega)^3]. \quad (26)$$

The case for face filling intermediate between half and full is indicated by the crosses in Fig. 7(a). Note that this is for fixed n_e, E_0 having been adjusted as above to preserve n_e. All of the moments shown in Fig. 7(a) reverse the sign of the moment with the sign of H so that with the exception of the filled-face case, all have a discontinuity in the moment at $H=0$. As will be shown (Fig. 8), this discontinuity is present only *at* $T=0$. For all finite T this discontinuity is removed, and the moment vanishes continuously at $H=0$.

The above developments for the moment, shown in Fig. 7(a), are essentially given by evaluating $M=-\sum \partial E_i/\partial H$, where the sum is over a constant number of states which are chosen to be the lowest ones for any given H, not necessarily the same states for all fields, as the break in OAB at A indicated. It is a calculation for an atomic Fermi-Dirac system when the central potential for all particles is given as parabolic. The results agree quite satisfactorily with what is known from atomic problems, i.e., for a filled shell (=face) the system is diamagnetic with $M\sim-(e^2H/6mc^2)\sum\langle r^2\rangle_{Av}$, which is essentially what Eq. (24) represents. For an unfilled shell the system *starts out* paramagnetic (unquenched orbital paramagnetism), to which is added Eq. (24), the above diamagnetic term. Since we have exact eigenvalues for the parabolic well, we know precisely what we have neglected and can, if we wish, estimate the validity thereof and at what point perturbation theory concepts fail.

We can extend our results to higher fields and temperatures. This we can do as follows and at the same time verify the above results in an independent manner.

The moment at $T=0$ is given by[4]

$$M_{T=0}=(\partial/\partial H)\int_0^{E_0} N(E)dE. \quad (27)$$

We recall that $N(E)$ is given by Eq. (3) with the numerical coefficients given by Eq. (4). Now in Eq. (4) we may substitute the dimensions which Fig. 1 takes on in the presence of a magnetic field. These are given

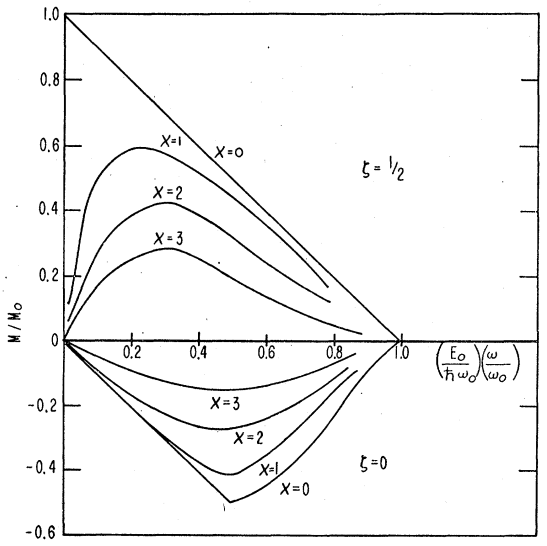

FIG. 8. Dimensionless magnetization at finite temperatures as a function of dimensionless field. The dimensionless temperature parameter for the different curves is $x=2\pi^2kT/\hbar\omega_0$. The positive values of moment are for the half-filled face whereas the negative moments are for the filled face.

exactly by Eq. (18) as

$$\begin{aligned} a&=E/2\hbar\omega,\\ b&=E/\hbar\omega_0,\\ c&=E/\hbar\omega(1+d),\\ c'&=E/\hbar\omega(1-d),\\ d&=(1+\omega^2{}_0/\omega^2)^{\frac{1}{2}}. \end{aligned} \tag{28}$$

This gives the following expressions for $N(E)$ and the moment, per unit volume (n_w wells), when one sums only the a_{qrs} corresponding to the normals (or near normals) to the principle faces of Fig. 1, i.e., only $a_{2j,j,j}$, $a_{2j,j,-j}$, $a_{-2j,-j,-j}$, $a_{-2j,-j,+j}$:

$$\begin{aligned} N(E)=&\left(\frac{n_w}{6}\right)\left(\frac{E}{\hbar\omega_0}\right)^3+2n_w\left(\frac{\omega_0}{\omega}\right)^2\sum_{j=1}^{\infty}\frac{(-1)^j}{(2\pi ij)^3}\\ &\times[-\exp(2\pi ijE/d\hbar\omega)+\tfrac{1}{2}(1+3\omega/2\omega_0)\\ &\times\exp[2\pi ijE/(d+1)\hbar\omega]+\tfrac{1}{2}(1-3\omega/2\omega_0)\\ &\times\exp(2\pi ijE/(d-1)\hbar\omega)+O(\omega^2/\omega_0{}^2)], \end{aligned} \tag{29}$$

$$\begin{aligned} M=&\left(\frac{\partial}{\partial H}\right)_{E_0}2n_w\hbar\omega\left(\frac{\omega_0}{\omega}\right)^2\sum_{j=1}^{\infty}\frac{1}{(2\pi j)^4}\\ &\times\left[-d\cos 2\pi j\left[\frac{E_0}{d\hbar\omega}-\frac{1}{2}\right]+\tfrac{1}{2}(d+1)\right.\\ &\times(1+3\omega/2\omega_0)\cos\left(2\pi j\left[\frac{E_0}{(d+1)\hbar\omega}-\frac{1}{2}\right]\right)\\ &+\tfrac{1}{2}(d-1)(1-3\omega/2\omega_0)\\ &\times\cos\left(2\pi j\left[\frac{E_0}{(d-1)\hbar\omega}-\frac{1}{2}\right]\right)\\ &\left.+O(\omega^2/\omega_0{}^2)\right]. \end{aligned} \tag{30}$$

Now this formula, Eq. (30), for the moment can be summed exactly by use of the Hurwitz formula,[8] which expresses the generalized Zeta function as a trigonometric series; and the Zeta function in turn can then be expressed as a polynomial.[9] Slightly different formulas are required for the range $0<(E_0/\hbar\omega_0)(\omega/\omega_0)<1/2$, 1/2 to 1, 1 to 3/2, etc. Different forms are also required depending on whether $E_0/\hbar\omega_0$ is an integer (filled face) or halfway between integers (half-filled face). In this way we have been able to verify exactly the expressions for the moment given in Eqs. (24), (25), (26), and have even carried them to still higher values of the field, i.e., $(E_0/\hbar\omega_0)(\omega/\omega_0)>1$. The general behavior of the moment is oscillatory, of decreasing amplitude and periodic in $(E_0/\hbar\omega_0)(\omega/\omega_0)$, as is indeed to be expected from the way in which the Fermi surface of constant energy catches and loses points in the lattice planes. Figure 7(b) gives the moment computed from Eq. (30), using the Hurwitz formula, for the somewhat artificial case for which E_0 (instead of n_e) is held fixed, so that here the "number of particles" is *not* preserved. It will be seen that *only* if $E_0/\hbar\omega_0=$an integer (filled face), or $E_0/\hbar\omega_0=$integer$+1/2$ (half-filled face), is fixing E_0 equivalent to fixing n_e, as previously mentioned.

By using only the largest term ($j=1$) of Eq. (30) to evaluate the moment, one can obtain a single analytic expression for the moment for all values of $(E_0/\hbar\omega_0)\times(\omega/\omega_0)$ (ω/ω_0 still $\ll 1$) which is a quite satisfactory approximation. This approximation for the moment per unit volume is

$$\begin{aligned} M=&(4n_w/(2\pi)^4)(e\hbar/2mc)\cos(2\pi E_0/\hbar\omega_0)\\ &\times\left\{-(\omega_0/\omega)^3\left(1-\cos\left[2\pi\frac{E_0}{\hbar\omega_0}\frac{\omega}{\omega_0}\right]\right)\right.\\ &\left.+\pi(E_0/\hbar\omega_0)(\omega_0/\omega)^2\sin\left(2\pi\frac{E_0}{\hbar\omega_0}\frac{\omega}{\omega_0}\right)\right\}. \end{aligned} \tag{31}$$

In Eq. (31), $E_0/\hbar\omega_0$ is an integer for a filled face [see Eq. (14), $T\to 0$], and an integer $+1/2$ for a half-filled face. Equation (31) is also plotted in Fig. 7(a).

Equation (31) is a better approximation for the moment for the filled face than for the half-filled face since the former has no discontinuity at $H=0$. For the filled face its chief deficiency is that it has twice too large a slope in the range $(E_0/\hbar\omega_0)(\omega/\omega_0)<1/2$, but otherwise it represents the amplitude and frequency quite satisfactorily. The one term ($j=1$) approximation for $N(E)$ which led to Eq. (31) is especially useful for evaluating the moment at higher temperatures and becomes there better and better since the terms with larger j are more heavily damped with temperature.

IV. THE MOMENT FOR FINITE TEMPERATURES

The case of a finite temperature can be handled in either of two ways. For $(\hbar\omega_0/kT)\gg 1$ one may include those exponential terms, previously dropped in Eq. (23), which correspond to lattice planes closest to the Fermi energy, just as in the case of the specific heat. For $(\hbar\omega_0/kT)\ll 1$ one may compute the moment from

$$M=(\partial/\partial H)\int_0^{\infty}N(E)f(E)dE, \tag{32}$$

and for $N(E)$ use the largest term ($j=1$) of Eq. (29), a procedure analogous to that which led to Eq. (31). These procedures give the following expressions for the

[8] See, for example, C. T. Whittaker and G. N. Watson, *A Course of Modern Analysis* (Cambridge University Press, London, 1935), pp. 267–269.

[9] Reference 8, p. 127.

moment per unit volume:

$$M(\zeta=\tfrac{1}{2})=(n_w/12)(E_0/\hbar\omega_0)^3(e\hbar/2mc)-(n_w/12)(E_0/\hbar\omega_0)^4(e\hbar/2mc)(\omega/\omega_0)$$
$$+n_w(E_0/\hbar\omega_0)^3(e\hbar/2mc)\left\{\frac{\exp[-(\hbar\omega_0/kT)]}{4}\left(\frac{E_0}{\hbar\omega_0}\frac{\omega}{\omega_0}\frac{\hbar\omega_0}{2kT}\right)^{-3}\left(1-\cosh\left[\frac{E_0}{\hbar\omega_0}\frac{\omega}{\omega_0}\frac{\hbar\omega_0}{kT}\right]\right)\right.$$
$$+\frac{\exp[-(\hbar\omega_0/kT)]}{4}\left(\frac{E_0}{\hbar\omega_0}\frac{\omega}{\omega_0}\frac{\hbar\omega_0}{2kT}\right)^{-2}\sinh\left(\frac{E_0}{\hbar\omega_0}\frac{\omega}{\omega_0}\frac{\hbar\omega_0}{kT}\right)$$
$$\left.-\frac{1}{8}\left(\frac{E_0}{\hbar\omega_0}\frac{\omega}{\omega_0}\frac{\hbar\omega_0}{2kT}\right)^{-2}\left(1+\exp\left[-\frac{E_0}{\hbar\omega_0}\frac{\omega}{\omega_0}\frac{\hbar\omega_0}{kT}\right]\right)+\frac{1}{8}\left(\frac{E_0}{\hbar\omega_0}\frac{\omega}{\omega_0}\frac{\hbar\omega_0}{2kT}\right)^{-3}\left(1-\exp\left[-\frac{E_0}{\hbar\omega_0}\frac{\omega}{\omega_0}\frac{\hbar\omega_0}{kT}\right]\right)\right\}, \quad (33)$$

valid if $(\hbar\omega_0/kT)\gg1$ and $(E_0/\hbar\omega_0)(\omega/\omega_0)<1$,

$$M(\zeta=\tfrac{1}{2})\simeq[(6n_e)^{4/3}/24](n_w/kT)(e\hbar/2mc)^2H \quad (33a)$$

provided also $(E_0/\hbar\omega_0)(\omega/\omega_0)\ll1$, and

$$M(\zeta=0)=-(n_w/12)(e\hbar/2mc)(\omega/\omega_0)(E_0/\hbar\omega_0)^4$$
$$+n_w(E_0/\hbar\omega_0)^3(e\hbar/2mc)\exp\left(-\frac{\hbar\omega_0}{2kT}\right)\left\{\sinh\left(\frac{E_0}{\hbar\omega_0}\frac{\omega}{\omega_0}\frac{\hbar\omega_0}{kT}\right)\Big/2\left(\frac{E_0}{\hbar\omega_0}\frac{\omega}{\omega_0}\frac{\hbar\omega_0}{2kT}\right)^2\right.$$
$$\left.-\sinh^2\left(\frac{E_0}{\hbar\omega_0}\frac{\omega}{\omega_0}\frac{\hbar\omega_0}{2kT}\right)\Big/\left(\frac{E_0}{\hbar\omega_0}\frac{\omega}{\omega_0}\frac{\hbar\omega_0}{2kT}\right)^3\right\}, \quad (34)$$

valid if $(\hbar\omega_0/kT)\gg1$ and $(E_0/\hbar\omega_0)(\omega/\omega_0)<1/2$. If $(\hbar\omega_0/kT)\ll1$, we have

$$M=\frac{4n_w}{(2\pi)^4}\left(\frac{e\hbar}{2mc}\right)\cos(2\pi E_0/\hbar\omega_0)\left[\frac{2\pi^2kT/\hbar\omega_0}{\sinh(2\pi^2kT/\hbar\omega_0)}\right]$$
$$\times\left\{-\left(\frac{\omega_0}{\omega}\right)^3\left(1-\cos\left[2\pi\frac{E_0}{\hbar\omega_0}\frac{\omega}{\omega_0}\right]\right)+\pi\left(\frac{E_0}{\hbar\omega_0}\right)\left(\frac{\omega_0}{\omega}\right)^2\sin\left(2\pi\frac{E_0}{\hbar\omega_0}\frac{\omega}{\omega_0}\right)\right\}. \quad (35)$$

In Eq. (35) $E_0/\hbar\omega_0$ is an integer for a filled face ($\zeta=0$) and an integer $+1/2$ for a half-filled face ($\zeta=1/2$).

Equations (33), (34), and (35) are plotted in Fig. 8, using interpolated values in the range of H and T where they begin to fail. Thus, Figs. 7 and 8 give a fair picture of the behavior of the moment for all values of temperature and field (providing still $\omega/\omega_0\ll1$). In general we see that as the fields and temperatures get larger, one may safely use Eq. (35), which indicates that the moment is heavily damped with increasing temperature; the amplitude of oscillation drops off, initially at least, like $1/H^3$. It can be shown that as the field gets still larger ($\omega/\omega_0>1$), the oscillations in moment ultimately become periodic in $1/H$ [instead of periodic in H, as in Eq. (35)] while the amplitude increases as H^3. This behavior is suggestive only of the de Haas-van Alphen effect. These conclusions are most easily reached using the general expressions for $N(E)$, Eq. (3), and the eigenvalues obtained from Eq. (18), where $\omega/\omega_0\gg1$. Since the eigenvalues are always linear in the quantum numbers, Fig. 1 is still qualitatively applicable, and no difficulty attaches to this procedure. The principle direction is now $(j, 0, 0)$ instead of $(2j, j, \pm j)$. One can also obtain the Landau diamagnetism throughout this development, but in the range of variables in which we are interested it is smaller than the moments we have derived by $O(\hbar\omega_0/E_0)$ so that it can be safely neglected.

V. DISCUSSION

The above derivations give a fairly complete picture of the magnetic and caloric properties of our model, consisting of n_w parabolic wells per unit volume, under the assumption that the Larmor frequency, ω, is somewhat less than the natural frequency, ω_0, of the well. Further, no great difficulty attaches to deriving the properties for $\omega>\omega_0$, mentioned above. Since all of our results have been presented in dimensionless form in the figures, they could be fitted approximately to real materials by adjusting the parameters m, n_w, n_e (or E_0), ω_0, about whose numerical values nothing has as yet been said. Evidently both diamagnetic and paramagnetic materials could be described, depending on whether the face closest to the Fermi surface is filled or not and also on whether we choose (perhaps somewhat unrealistically) to keep E_0 (as opposed to n_e) fixed for

weak fields. Our model is quite impartial in that it has no preference for either diamagnetic or paramagnetic behavior. For n_e fixed (Fig. 7(a)) the initial behavior with H is paramagnetic for all fillings of a face except the unique case of one exactly full, which is diamagnetic. For E_0 fixed (Fig. 7(b)) the initial behavior is in general diamagnetic, with the exception that for an exactly half-filled face it is initially paramagnetic. Thus for $\zeta=0$ and $\zeta=1/2$, E_0 fixed and n_e fixed agree, and for these cases only.

The model has considerably more versatility than one might expect would be provided by the addition of only one more parameter to the three initially needed for an Einstein lattice model. It should be noted that this versatility depends quite intrinsically on the discreteness and degeneracy of the levels, as well as on the numbers of particles used to fill them. All this is quite in keeping with our conclusions in previous studies[4] about the significance of discreteness in energy levels for magnetic properties. The versatility of this simple and computable model also may throw some light on the diverse results[10–12] of previous calculations on the cylindrical box, especially in weak fields, since evidently by changing the numbers of particles by a relatively small amount, fixing n_e, or E_0, we get totally different results for the problem at hand.

For the purpose of clarity we would like to give one more figure which will render the comparison with real materials more illuminating.

For the filled-face case we have plotted in Fig. 9 contours of constant μ (permeability) in a dimensionless H, T plane. This figure should be studied in conjunction with the filled-face specific-heat curves of Figs. 4 and 5. drawn to the same temperature scale. Since the magnetic induction $B=\mu H=H+4\pi M$, then $\mu=1+4\pi M/H$; and since we have M as a function of H and T [Eqs. (34) and (35), or Fig. 8], we may evaluate μ for a network of dimensionless H, T values and then by interpolation draw contours of constant μ. This is done in

TABLE I. Model parameters for superconductors.

Element	H_0 gauss	T_c °K	A cc	m/m_e (lower limit)	Number of particles per atom (lower limit)	$10^{-8}\times$number of particles per well (lower limit)
Cd	28	0.56	13.0	1.5	0.023	8.9
Zn	53	0.90	9.2	1.6	0.033	6.8
Tl	170	2.4	17.2	1.6	0.20	3.7
In	275	3.4	15.7	1.7	0.32	3.0
Sn	310	3.72	16.3	1.8	0.39	3.3
Hg	420	4.17	13.9	2.2	0.55	3.4
Pb	800	7.2	18.3	2.2	1.38	2.5
Ru	46	0.47	8.3	3.7	0.061	17.8
Os	65	0.71	8.4	3.1	0.073	12.6
Al	106	1.20	10.0	2.6	0.12	8.4
Ta	980	4.4	10.9	5.9	2.71	6.2
V	1200	5.13	8.4	6.1	2.64	5.9
Nb	2600	8.0	11.0	8.2	9.16	5.3

[10] M. F. M. Osborne and M. C. Steele, Phys. Rev. **86**, 247 (1952).
[11] R. B. Dingle, Proc. Roy. Soc. (London) **A216**, 118 (1953).
[12] W. Band, Phys. Rev. **91**, 249 (1953).

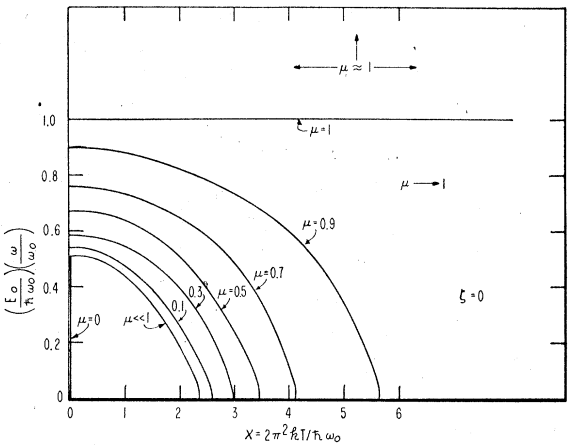

FIG. 9. Contours of constant permeability μ in a dimensionless H, T plane for the diamagnetic (filled-face) case. The parameters are adjusted so that when $x=0$, $\mu=0$ for the dimensionless field ranging from 0 to 1/2.

Fig. 9, where we have chosen $\mu=0$ as our origin at $T=0$. This corresponds to adjusting the slope OA of Fig. 7(a) [Eq. (24)] so that the material can just drive out the applied field at $T=0$. [Cf. Eq. (37).]

The similarity between the contours of constant μ and the critical field curves of superconductors is most striking. If we fit the H and T intercepts of the $\mu=1/2$ contour (inside this contour our model is strongly diamagnetic, outside essentially normal, $\mu\sim1$) to the parameters H_0 and T_c of a real superconductor, we can evaluate some of the parameters m, n_e, n_w, B of our model. Note also that this contour, $\mu\simeq1/2$, has a temperature intercept ($x=2\pi^2kT/\hbar\omega_0\sim3.5$) at approximately the same point where the corresponding specific-heat curve has an anomalous bump. If either the field or temperature is increased outside the $\mu=1/2$ contour, the diamagnetism disappears and the specific heat becomes linear, all quite in agreement with the behavior of a superconductor. If we fit the observed linear specific heat to that of our model, we obtain an additional condition on our parameters. This fitting process is carried out in the next section (Table I).

The comparison of our model to a real paramagnetic or ferromagnetic material is not so happy as is the case with superconductors. Indeed, this is not surprising, since we have nowhere introduced electron spin, conventionally regarded as essential to a description of such materials. (For superconductors on the other hand, the experiments of Kikoin and Goobar[13] on the gyromagnetic ratio of superconductors are indicative that the diamagnetism of superconductivity is not connected in any direct way with electron spin.) A description of ferro- or paramagnetic materials is nonetheless interesting, if we focus attention on certain gross properties and ignore others.

[13] I. K. Kikoin and S. V. Goobar, J. Phys. (U.S.S.R.) **3**, 333 (1940).

Let us first point out where the diamagnetic and paramagnetic contributions to our various expressions for the moment arise. Terms in ω^2 in the energy, Eq. (19) from *all* the states within the Fermi surface contribute to the diamagnetism. Paramagnetic terms arise from an unbalance in the *number* of states with negative as opposed to positive values of l [term in $lh\omega$ in Eq. (19) or (20)]. We have seen that for the filled face these balanced exactly so long as $(E_0/h\omega_0)(\omega/\omega_0)<1/2$, whereas for the half-filled face there was, for finite $H[(E_0/h\omega_0)(\omega/\omega_0)<1]$, an unbalance of one $(-l)$ face (*DBC* of Fig. 1), and as H increased [beyond $(E/h\omega_0)\times(\omega/\omega_0)=1$], the number of $-l$ states increased while the number of $+l$ states decreased. The net effect of the sum of pure para- and diamagnetic terms gives an oscillating moment arising from the inclusion and exclusion of states within the Fermi surface as it cuts an increasing number of lattice planes.

Now note that the paramagnetic contribution of any given state to the moment is independent of H [i.e., $(\partial/\partial H)lh\omega$] so that any *changes* in paramagnetic contribution must come from *changes* in the *occupancy* of states. Hence, in the *absence* of any small interaction (usually assumed present to permit an approach to thermodynamic equilibrium) which will allow particles to move from one state to another, the paramagnetic contribution to the moment will remain a constant.

This aspect of our model possibly gives a clue to the explanation of frozen-in moments in superconductors (for case $\zeta=0$) and to the existence of remanence on reduction of H after saturation for a paramagnetic salt which becomes ferromagnetic at $T=0$ (described on the basis of the $\zeta=1/2$ case). It can easily be seen that the unbalance of $+$ and $-l$ present in our model for large $H[(E/h\omega_0)(\omega/\omega_0)>1/2$ or 1 for $\zeta=0$ or $\zeta=1/2]$, if preserved at $H=0$ (not the state of thermodynamic equilibrium), will always give a residual moment in the absence of a field. This would correspond to moments paralleling the xxx curves of Fig. 7(a) as the field H is removed.

With this understanding of the effect of the absence of interactions which would allow states to change their occupancy, our model can have, at $H=0$, $T>0$, a remanent moment of either sign depending on the sign of the field "last seen." This is *not* a property of thermodynamic equilibrium.

We may also fit our model (with of course a different set of parameter values) at least roughly to the properties of a paramagnetic salt with zero Curie temperature. We observe that in the low temperature, low field regions of Fig. 8, or Eq. (33a), the moment for the case of a half-filled face is given by an expression of the form $M\sim CH/T$ and approaches a "saturation" value, whereas the specific heat (Fig. 5) has a thin spine which broadens with increasing field. At $T=0$ our model may develop a remanent moment, $\leq M_{\text{sat}}$ (Fig. 7). This is approximately the behavior of a paramagnetic salt with a zero Curie temperature. Thus, the parameters of our model can be evaluated by fitting the zero-point entropy, the saturation moment, and the Curie constant to a real material. Evidently the model will fail at sufficiently high fields and temperatures as the model then has a linear in T specific heat and a moment which vanishes for sufficiently large fields [Eq. (58)] in disagreement with available experiment.

Table II gives a set of values of parameters fitting this aspect of the model to a paramagnetic salt. In all of this fitting process the significant combination of parameters includes those which give the size of the well, the number of particles per well, and the numbers of particles per atom of material, rather than the parameters (B, m, n_w, n_e) with which the model was set up.

VI. EVALUATION OF THE PARAMETERS OF THE MODEL

Let us now consider the numerical problem of fitting the parameters of our model to real materials. Instead of the set B, m, n_e (or E_0), n_w we shall use equivalent sets which will perhaps provide slightly more physical insight. Superconductivity is believed to be an example of cooperative phenomena between many electrons (or atoms). Hence, the radius of the well, $R=(2E_0/B)^{\frac{1}{2}}$, or the distance from the center which corresponds to E_0, is a measure of the distance over which this cooperation is effective. The number of particles per atom, $n_e n_w A/N_{\text{Avogadro}}$, is in some sense a measure of the extent to which each atom contributes to the cooperation, whereas n_e is a measure of the effective number of cooperating particles. That elusive parameter, the ratio of the mass to the electronic mass m/m_e, is in some sense an indication of the extent to which the electrons are not free, and $h\omega_0$ is a measure of the cooperative interaction energy. We shall, as far as we can, express the above in terms of observable quantities (H_0, T_c, γ_e, the electronic specific heat, M_{sat}, Curie constant C, T_{Curie}, A, the atomic volume) and tabulate values for specific materials.

TABLE II. Model parameters for paramagnetic salts.

Salt	Curie constant C (molar)	$M_{\text{sat.}}$ (molar)	S_0 (molar) (ergs/mol deg)	$\frac{S_0 C}{M_s^2}$	n_w	n_e	Upper limit on λ-well size (cm)	$H(M=0)$ Lower limit (gauss)
$KCr(SO_4)_2\cdot 12H_2O$ $A=273$ cc	1.86	$3N_{Av}\beta$	1.1×10^8	0.75	2.1×10^{21}	6.7	5.0×10^{-8}	9.6×10^7
$Gd_2(SO_4)_3\cdot 8H_2O$ $A=248$ cc	7.83	$7N_{Av}\beta$	1.7×10^8	0.89	0.90×10^{21}	38.9	6.4×10^{-8}	5.5×10^7

A. Superconductor

Consider first the case of a filled face, fitted to a superconductor. The condition for equality of the specific heats when linear is

$$\frac{\pi^2 k^2}{6}\frac{(E_0)^2}{(\hbar\omega_0)^3}n_w A=\gamma_e, \tag{36}$$

where $\gamma_e T$ is the linear term in the electron specific heat of one g atom in ergs/mol (°K). A second condition is that the permeability μ be 0 at $T=0$. From Eq. (24), setting $H+4\pi M=0$, we find

$$1=(\pi/12)(1/\omega_0)(he^2/m^2c^2)(E_0/\hbar\omega_0)^4 n_w. \tag{37}$$

Two more conditions are obtained by identifying the $\mu=1/2$ contour, Fig. 9, with the critical field curve and equating its intercepts at $H=0$ and $T=0$ to the experimental observed values for these parameters. This gives

$$(2\pi^2 kT_c/\hbar\omega_0)\simeq 3.5, \tag{38}$$

$$(E_0/\hbar\omega_0^2)(eH_0/2mc)\simeq 0.67. \tag{39}$$

Two additional conditions are given by the following considerations. We would like to identify the size of the well, $(2E_0/B)^{\frac{1}{2}}$ with the penetration depth, λ_0 at $T=0$. Evidently if we take a "physical sample" of our model so small that it cannot contain even one full-sized well, its diamagnetic properties will certainly be diminished if not entirely destroyed. This is also the case with a real superconductor. So we have, plausibly, at least,

$$\lambda_0=(2E_0/B)^{\frac{1}{2}}. \tag{40}$$

Finally, for the "physical consistency" of our model, since we have treated each well as not in interaction with any other well, we must have the condition that the volume occupied by each well is less than the space available $(1/n_w)$ to each well. This requires

$$(4/3)\pi(2E_0/B)^{\frac{3}{2}}<1/n_w. \tag{41}$$

The equalities (36)–(40) are *not* sufficient to determine all the parameters of our model but instead only three different combinations of them, ω_0, $n_w m^2$, and n_e/m^3. This situation is similar to that for the Einstein lattice model. Combined with the inequality Eq. (41), we can get separate inequalities on all of them. Elimination of all parameters between (36)–(40) will give conditions on the experimental observables *alone*, which are, pleasantly enough, in agreement with observation so that our model is a consistent one. ζ was a "bonus parameter" consequent to number theory since as n_e varies over a small range $(E_0/\hbar\omega_0$ from p to $p+1)$, ζ takes any value we please between 0 and 1.

Choosing as model parameters, $\omega_0=(B/m)^{\frac{1}{2}}$, $n_e=\frac{1}{6}(E_0/\hbar\omega_0)^3$, m, n_w, we can write Eqs. (36) to (41) as

$$\frac{\pi^2}{6}k^2\frac{(6n_e)^{\frac{2}{3}}}{(\hbar\omega_0)}n_w A=\gamma_e, \tag{42a}$$

$$1=(\pi/12)(\hbar/\omega_0)(e^2/m^2c^2)(6n_e)^{4/3}n_w, \tag{42b}$$

$$(2\pi^2)kT_c/\hbar\omega_0=3.5, \tag{42c}$$

$$\frac{(6n_e)^{\frac{1}{3}}}{\omega_0}(eH_0/2mc)=0.67, \tag{42d}$$

$$\lambda_0^2=\frac{2(6n_e)^{\frac{1}{3}}}{\omega_0 m}\hbar, \tag{42e}$$

$$(4\pi/3)(2\hbar/\omega_0 m)^{\frac{3}{2}}(6n_e)^{\frac{1}{2}}n_w<1. \tag{42f}$$

ω_0 is determined by Eq. (42c). Equations (42b, c, and d) give

$$n_w m^2=(12/\pi)(3.5\hbar/2\pi^2 kT_c)^3\frac{e^2H_0^4}{\hbar c^2 2^4(0.67)^4}; \tag{43}$$

(d) and (c) give

$$(n_e^{\frac{2}{3}}/m^2)=(0.67/6^{\frac{1}{3}})(c/eH_0)(4\pi^2 kT_c/\hbar\ 3.5)^2; \tag{44}$$

whereas (a) and (b) give

$$(n_e^{\frac{2}{3}}/m^2)=(2/6^{\frac{2}{3}})(c^2 A\pi k^2/\hbar^2 e^2\gamma_e). \tag{45}$$

This is as far as we can go without the use of Eq. (42f). [Equation (42e) is also a function of $n_e^{\frac{1}{3}}/m$.] However, equating the last two expressions [Eqs. (44) and (45)] for the combination $n_e^{\frac{2}{3}}/m^2$ gives

$$(T_c^2/H_0^2)(\gamma_e/A)=(3.5)^2/(0.67)^2 8\pi^3=1/9.1. \tag{46}$$

All other parameters and physical constants cancel. Equation (46) is simply the thermodynamic relation derived with the aid of the parabolic law, Rutger's equation, and the absence of a linear term in the superconducting specific heat.[14] Evidently the correct numerical coefficient 2π instead of 9.1 could be obtained by choosing a somewhat smaller permeability contour (say $\mu=0.3$) as representative of the critical field curve. Our model is evidently a consistent one thermodynamically.

A second relation in which the parameters of the model disappear can be obtained by eliminating $n_e^{\frac{1}{3}}/m$ between Eqs. (42d) and (e) [equivalent relations could be obtained by using Eq. (42e) with Eq. (44) or (45)]. This gives for the penetration depth

$$\lambda_0=(1.6)(\hbar c/eH_0)^{\frac{1}{2}}. \tag{47}$$

This relation is plotted in Fig. 10 as the solid curve with experimental points from the sources indicated. The trend with H_0, as well as the absolute values, is surprisingly well represented in consideration of the simplicity of the model. Evidently the theoretical coefficient in Eq. (47) is uncertain to at least a factor of 2. A relation equivalent to Eq. (47) can also be derived

[14] See, for example, D. Shoenberg, *Superconductivity* (Cambridge University Press, London, 1952), p. 64, for a derivation of the functional relation (to a numerical constant) given by Eq. (46) in the present paper.

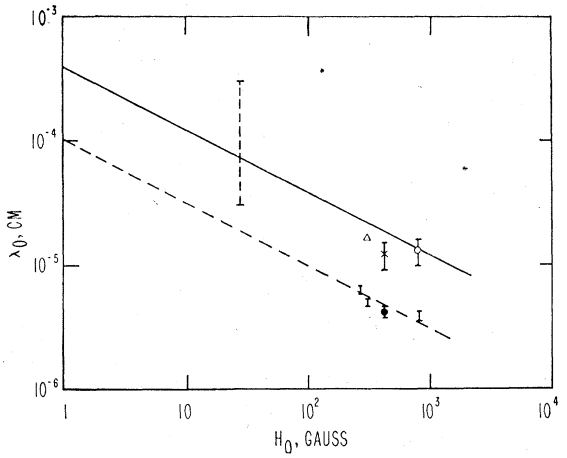

FIG. 10. Logλ_0 *vs* logH_0. The experimental points are taken from the following sources: I, (Pb, Sn, In) J. M. Lock, Proc. Roy. Soc. (London) **A208**, 391 (1951). ●, (Hg) E. Laurmann and D. Shoenberg, Proc. Roy. Soc. (London) **A198**, 560 (1949). o, (Pb) M. C. Steele, Phys. Rev. **78**, 791 (1950). ×, (Hg) Appleyard, Bristow, London, and Misener, Proc. Roy. Soc. (London) **A172**, 540 (1939). △, (Sn) N. E. Alekseevsky, J. Phys. (U.S.S.R.) **4**, 401 (1941). ⁞, (Cd) M. C. Steele and R. A. Hein, Phys. Rev. **87**, 908 (1952). The dashed curve fitting the Cambridge data corresponds to a constant of 0.41 instead of 1.6 in Eq. (47).

from London's concept[15] of superficial currents whose elemental charges each carried an angular momentum of $\hbar$.

An expression for the number of particles per atom $n_e n_w A/N_{\text{Avogadro}}$ can be obtained from Eqs. (43) and (44) or (45). This is

$$n_w n_e A/N_{\text{Av}} = (mA/N_{\text{Av}})(1/\pi\ 0.67)(cH_0/e\hbar). \quad (48)$$

Finally Eq. (42f) with Eqs. (43) and either (44) or (45) can be used to obtain the following inequality on the mass,

$$m > \frac{(3.5)^{3/2}}{(0.67)^{5/4}\pi^3}\,\frac{\hbar^{7/4}e^{1/4}H_0^{5/4}}{(2)^{\frac{1}{2}}(kT_c)^{3/2}c^{1/4}}. \quad (49)$$

This in turn can be used to give lower limits on the number of electrons per atom [Eq. (48)] as well as a lower limit on n_e, and an upper limit on n_w.

Values for some typical superconductors are given in Table I.

In general it will be observed that the number of particles per atom ranges from 1/50 to 10, with masses slightly in excess of the electronic mass. Values of, or limits on, the other parameters ω_0, B, E_0, and n_w can easily be computed, but it did not seem worthwhile until their significance could be more clearly established. The three given in Table I, together with ω_0 (which is determined by T_c alone) are sufficient to determine the model completely.

[15] F. London, Revs. Modern Phys. **17**, 310 (1945); M. C. Steele and M. F. M. Osborne, Phys. Rev. **91**, 1281 (1953).

B. Paramagnetic Salt

In attempting to fit our model for $\zeta=1/2$ to a paramagnetic salt, we observe that in the range of validity of Eq. (33a) [Fig. 8 for $(E_0/\hbar\omega_0)(\omega/\omega_0)\ll 1$], the susceptibility (per cc) is approximately

$$\chi = C/T = \eta n_w (n_e^{4/3}/k)(e\hbar/2mc)^2/T, \quad (50)$$

where $\eta = 6^{4/3}/24$. This determines the Curie constant C. Equation (25) gives for $M_{s,0}$ the saturation moment per cc at $T=0$,

$$M_{s,0} = n_w n_e e\hbar/4mc. \quad (51)$$

Finally, if we define an experimental quantity $S_0 = \int (Cv/T)dT$, the zero-point entropy per cc, in which the range of integration is over the experimental specific-heat peak of a paramagnetic salt, we have

$$S_0 \simeq k n_e^{\frac{2}{3}} n_w (\ln 2/2) 6^{\frac{2}{3}}. \quad (52)$$

This is obtained from[16] $S_0 = n_w k \ln G$, in which G is the number of ways a face may be half-filled according to Fermi statistics. From Eqs. (50), (51), and the inequality Eq. (41), we obtain the following expressions for our model parameters in terms of experimental quantities. $\beta = e\hbar/2mc$ is the Bohr magneton if $m=m_e$.

$$n_w = (M_{s,0}^4\beta^2/k^3C^3)2^4\eta^3, \quad (53)$$

$$n_e = k^3C^3/M_{s,0}^3\beta^3 2^3\eta^3, \quad (54)$$

$$\lambda < (3/4\pi)^{\frac{1}{2}}/n_w^{\frac{1}{3}} = (3/4\pi)^{\frac{1}{2}} kC/M_{s,0}^{4/3}\beta^{2/3}2^{4/3}\eta. \quad (55)$$

C and $M_{s,0}$ are for 1 cc in these expressions. Moreover, we have a relation which the model requires between the observed quantities only, just as was the case for superconductors, Eq. (46). This is obtained from Eqs. (50), (51), and (52). If all experimental quantities are on a molar or cc basis, this gives

$$S_0 C/M_{s,0}^2 \simeq 2\eta 6^{\frac{2}{3}} \ln 2 = 2.1. \quad (56)$$

A free spin theory[17] of paramagnetism of N_{Av} particles of spin s, has for this numerical constant

$$S_0 C/M_{s,0}^2 = \tfrac{1}{3}[s(s+1)/s^2] \ln(2s+1). \quad (57)$$

This is a slowly varying function of s, which our crude theory has approximated by the too large constant 2.1. The disagreement is quite analogous to that found in Eq. (46) for superconductors.

There is a field $H(M=0)$ at which the moment vanishes for our paramagnetic model. We can determine a lower limit for this from the condition $(E_0/\hbar\omega_0^2) \times [eH(M=0)/2mc] = 1 = [(6n_e)^{\frac{1}{3}}/\omega_0][eH(M=0)/2mc]$, Eq. (55) and Eq. (42e) for λ^2,

$$H(M=0) > 16\eta^2(8\pi/3)^{2/3}(c\hbar/e)(M_{s,0})^{8/3}\beta^{4/3}/k^2C^2. \quad (58)$$

Our model is good only at fields much less than this.

Evidently four independent parameter combinations

[16] R. C. Tolman, *Principles of Statistical Mechanics* (Clarendon Press, Oxford, 1938), p. 370.

[17] Reference 3, p. 581.

cannot be determined in this case either. A limit on the combination $\omega_0 m$ may be obtained from Eqs. (55), (54), and (42e). m is taken as the electronic mass for computing numerical values from Eqs. (52–58) in Table II, lacking other criteria to determine it. These results are tabulated below for two typical paramagnetic salts.

VII. CONCLUSION

It may appear as rather surprising that so simple a model of spinless electrons in a solid can be made to develop so great a variety of properties as those manifested by superconductors and paramagnetic salts. We should like to comment on the physical reasons underlying this versatility of the model since these comments may be suggestive of where to look for the explanation, especially of superconduction, from a more fundamental standpoint. We would first like to point out that if a system is obeying Fermi statistics and kT is greater than the spacing of electron levels, then the thermodynamic properties are essentially determined by the average density of levels in the neighborhood of the Fermi energy and are quite insensitive to the properties of the levels for larger or smaller energies. If, on the other hand, kT is less than the spacing, then the thermodynamic properties are determined by the density and degree of degeneracy of levels closest to the Fermi energy even though those levels may be more remote in energy than kT. In summary, for Fermi statistics, thermodynamic properties are determined by those levels closest to the Fermi energy; if there are levels closer than kT, specifying the properties of the levels in a range of order kT is sufficient to determine the thermodynamic properties.

Now our model has just the property that by adjusting its parameters one can vary the *average* density of levels, their degeneracy, and their spacing in an almost arbitrary manner. To show this we have plotted schematically in Fig. 11 the density of levels per cc $=n_w g(E)$ as a function of energy E and for different values of the magnetic field. Any dimension in abscissa of this figure can be made large or small compared to kT by adjusting the parameters of the model ω_0, m (or their equivalent). The ordinate can be adjusted to any size by varying, among other parameters, n_w and n_e. The area of each triangle is n_w times the number of points in the faces of Fig. 1. Their bases are in length proportional to H. The triangles begin to overlap at $(E/\hbar\omega_0)(\omega/\omega_0)=1/2$. We have seen that by half-filling a face we place the Fermi energy at the vertex of a triangle. When the face is filled, the Fermi energy falls halfway between triangles, i.e., in a region of no-energy levels if the field is weak. Hence, by adjusting the parameters of the model, we may produce any effective density, spacing, and degeneracy we please in the neighborhood of the Fermi energy and then compute unambiguously the effect of a magnetic field since the energy levels are always linear in the quantum numbers. The triangles themselves are actually composed of δ functions, spaced $\hbar\omega$ apart. This property of the model gives a flexibility we have not utilized since it becomes significant only when $kT<\hbar\omega$. We have called this condition (Sec. III) effectively $T=0$.

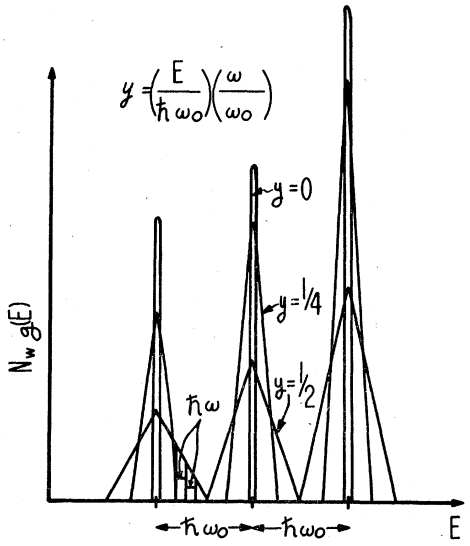

FIG. 11. Schematic density of levels per cm³ as a function of energy, for different fields.

For some of the cases we considered, not all of the dimensions of Fig. 11 are significant. This corresponds either to the fact that we could not compute all our parameters unambiguously or to the fact that our model failed when H or T exceeded certain values.

We should now like to discuss just how sensitive to imperfection are the properties of our model, especially when considered as a superconductor. We have assumed n_w isotropic wells per unit volume, each containing just the proper number of particles to fill completely the "faces" of its energy surface in quantum-number space. We have already seen that a shift from filled to half-filled face or a variation of the number of particles by 1 part in $n_e^{\frac{1}{3}}$ is sufficient to shift the properties from an intense diamagnetism to an equally intense paramagnetism. In other words, the number of particles in each well has to be fixed to better than 1 part in 10^3, judging by the figures in Table I.

Secondly, we observed that if the wells are slightly anisotropic, this condition has the effect of tilting the energy surfaces of Fig. 1 (for no field) out of parallelism with the 2, 1, 1 and 2, 1, -1 planes. If sufficient to tilt the Fermi surface enough to cut a lattice plane, it will destroy the degeneracy and spacing properties which provided the diamagnetism, or paramagnetism, and specific heat anomalies. An anisotropy (say in ω_0) as small as one part in $n_e^{\frac{1}{3}}$, ($\sim$0.1 percent by Table I) is sufficient to destroy these properties. Such an anisotropy would be equivalent to having triangles instead of δ functions, for $y=0$ in Fig. 11.

Another condition to which our model is sensitive is the degree of overlap of wave functions in one well with

neighboring wells or the extent to which the inequality (41) is obeyed. The effect of nearest neighbor interactions will be to broaden the degenerate levels in a given face into bands. If these bands overlap (broadening $>\hbar\omega_0$), the degeneracy essential to our magnetic and specific heat behavior will be destroyed.

Evidently our model is rather sensitive to physical imperfections; or, to express the idea in another way, the model must be "well ordered" to the above degree throughout the specimen.

One consequence of the above close specifications of the parabolic well model is that the moment oscillates with H and with decreasing amplitude ($\sim 1/H^3$) for fields greater than the critical field [$(E_0/\hbar\omega_0)(\omega/\omega_0)>1$, Sec. III]. The specific heat anomaly and the perfect diamagnetism were consequences of only the two degenerate faces closest to the Fermi energy, whereas the above oscillations require this high degeneracy for additional inner and outer faces.

Berlincourt and Steele[18] have performed experiments with tin to test the prediction of additional oscillations in the magnetic moment of a superconductor at fields above the critical field. Their results showed that at fields above H_0 (the critical field) the moment of tin was less than 10^{-3} times the maximum superconducting moment, whereas the above theory indicates the possibility of a paramagnetic moment 10^{-1} times the maximum superconducting moment.

The negative experimental results require the additional postulate that our wells, or their filling, are rendered imperfect by at least the small amounts specified above for fields appreciably greater than the critical field. This small modification of the well structure is quite analogous, but on a much less drastic scale, to the modification by melting of an Einstein model for a solid to a liquid.

The problem of the conductivity of our model is one which remains to be investigated. However, a few qualitative remarks as to what one should and should not ask of the model are perhaps not out of place. One could certainly compute a zone structure for n_w wells distributed in a "superlattice" by Heitler-London methods, construct progressive wave solutions from the well-type wave functions and calculate the resistance from a postulated interaction with the lattice, all along conventional lines. The problem would not be to show that the resistance $\rightarrow 0$ as $T\rightarrow 0$, since this would follow for any perfectly periodic structure. Rather one should show that in the absence of a magnetic field the resistance for the filled-face case approached zero much faster than that for the half-filled face and that both became "normal" when H and T exceeded certain values.

The behavior of the density of levels for one well and the specific heat indicate that this latter property should not be overly difficult to realize. To obtain the former would require a knowledge of the scattering between a large number of (number of points in a face of Fig. 1) overlapping zones about which we would not care to hazard a guess without further calculation.

Closely connected with the problem of resistance is that of the conservation of flux of a multiply connected superconducting body. Since this conservation of flux is also not a thermodynamic property (i.e., depends on path in H, T plane), we have not attempted to explain it in this paper.

We can also emphasize certain characteristic features which it has that should be sought from a more fundamental basis. This is its outstanding property, that the degeneracy and filling of the wells is such that no shift in population or distribution of the particles can occur until the field reaches a critical value. The merit of the model is that this field can be computed without perturbation theory. The actual size of the well is physically unimportant except in so far as it can be identified with the penetration depth. Hence, our model tells us that we must find a computable situation where the actual wave functions spread over many atoms and the energy levels are sufficiently degenerate so that the spacing between different degenerate levels is $\sim(2\pi^2 kT_c/3.5)$. As we saw from Fig. 3, boxes of the proper size[19] alone are not sufficient; the degeneracy and filling must also be taken into account. From the recent work of Slater[20] we know that certain types of exact wave functions do indeed extend over many atoms just in the range of energy of the conduction bands. Hence, the problem resolves itself if it can be shown that one can realize sufficiently extended wave functions, and at the same time with a sufficient degree of degeneracy and spacing to provide a situation equivalent to that provided by the n_w parabolic wells. When and if this is done (and in the presence of a magnetic field), one will have a theory of the superconducting state. One will *not* have a theory of the superconducting transition. The model can only tell when it (like Einstein's lattice with large oscillations) will fail and presumably be normal. Indeed the success of our model suggests that one might use as starting wave functions the wave functions of our n_w parabolic wells (certainly as complete a set as any other) and endeavor to show that these can be used with perturbation theory to represent the electronic wave functions in a lattice of atomic periodicity. Whether it can be shown that the perturbation of the electrons by the lattice, weakening with diminishing temperature, is sufficient to permit such a clumping of the electrons as our n_w wells require and Slater's exact calculations show can happen ideally, remains to be determined.

Finally, we should like to give a justification or at

[18] T. G. Berlincourt and M. C. Steele, Phys. Rev. **91**, 215 (1953).

[19] Small boxes to provide a model for a superconductor have been considered also by J. C. Slater, Phys. Rev. **52**, 214 (1937) and F. Hund, Ann. Physik **32**, 102 (1938).

[20] J. C. Slater, Phys. Rev. **87**, 807 (1952).

least a precedent for our model, not only as a superconductor but as an admittedly crude representation of magnetic solids. We have replaced the multitudinous interactions of the electrons both with each other and the lattice, including spin, by an equivalent effective potential. It is rather pleasant and encouraging that just one model is sufficient to describe approximately a rather wide variety of properties. The parabolic potential is admirably suited to the purpose although at least one other, the Coulomb well, might serve as well.

Now this assumption of an equivalent potential to replace a complex interaction has had ample precedent in the past although the path to justification is often tortuous and long delayed. The Einstein lattice model is the one we have followed. As other examples we may cite the Lennard-Jones potential for gas molecules and Hooke (and other) forces between atoms in a solid, both of which were proposed long before there was any quantum mechanical theory of their origin. Similar examples of more recent date are the Weiss internal field and theories of the heavier nuclei, justification for which is not yet complete. These examples, we hope, give some precedent for our otherwise arbitrary assumption of parabolic wells.

PHYSICAL REVIEW VOLUME 92, NUMBER 6 DECEMBER 15, 1953

Anelasticity of Quartz

RICHARD K. COOK AND ROBERT G. BRECKENRIDGE
National Bureau of Standards, Washington, D. C.
(Received March 20, 1953)

By means of the piezoelectric effect, measurements have been made of the variation with temperature of (1) the Q of quartz bars executing free acoustical oscillations in torsion, and (2) the equivalent series electrical resistance of bars driven at their natural frequencies of longitudinal acoustical oscillations. For each of the bars studied, it was found that the internal dissipation had a maximum value at a temperature between room temperature and the quartz inversion temperature of 573°C. Measurements of resistance were made on one bar at several different frequencies. These data showed that part of the dissipation was due to a relaxation effect, whose decay time varied with temperature according to an Arrhenius equation. An activation energy of 22 kcal/mole and a relaxation-time constant of 2×10^{-14} sec were deduced from the data, which showed also that the fraction of energy lost during each sinusoidal cycle of strain was independent of the frequency of vibration. Estimates of the activation energies and relaxation-time constants were deduced for the other bars measured. In one case, the dissipation was due to the migration of gold atoms from the electrodes into the quartz lattice.

I. INTRODUCTION

WHEN a solid material is set into free vibration in one of its normal modes, the amplitude of the vibration decays exponentially with time. This happens even in the absence of external losses through either acoustic radiation into the air or other medium in which the solid is immersed, or through transmission of vibrational energy through the supports of the solid. The conversion of the ordered vibrational motion into disordered thermal motions of the molecules has been called "internal friction" or "internal dissipation", and more recently has been named "anelasticity". A summary of measurements on anelastic effects in metals, and a discussion of the mechanisms which give rise to anelasticity, are given in Zener's book,[1] where many of the formal analogies to dielectric theory are pointed out.

To the best of our knowledge, there have been no previous reports on researches into anelastic effects in quartz or other piezoelectric materials. Such effects in quartz are technologically important wherever quartz crystals are used either for frequency control of oscillators, or for electric-circuit filters. Measurements of anelastic effects in quartz, and in other piezoelectric materials, are readily made with electrical techniques. This is because the mechanical motions of a piezoelectric material cause electrical effects through the electromechanical coupling in the material. The most important information concerning the mechanism in any particular piece of material can be obtained from a study of the variation of anelastic effects with temperature and frequency.

A convenient measure of the internal friction is the Q of a freely vibrating system. Suppose the vibration as a function of time t is representable by $\exp(-\alpha t)\sin(2\pi ft)$, where α=damping coefficient of the damped vibration and f=frequency. The Q is then given by $Q=\pi f/\alpha$.

Another convenient measure of the internal mechanical friction for a piezoelectric material, such as quartz, is the electrical resistance R_1 which appears in the equivalent circuit of the crystal (see Fig. 1) when it is driven electrically at frequencies near a mechanical resonance frequency. It can be readily seen from Fig. 1

[1] C. Zener, *Elasticity and Anelasticity of Metals* (University of Chicago Press, Chicago, 1948).